Chapter-5

Summary

The Diels-Alder reaction (DA) involves [4+2] cycloaddition of a conjugated diene with dienophile. In the synthetic organic chemistry, the DA reaction occupies a very prominent place because with the help of this reaction, by using appropriately substituted diene and dienophile, up to four stereogenic centres can be introduced in one step with high stereo- and regio-selectivity. Use of heteroatoms in both, the diene and the dienophile broadened the horizon of the DA reactions and such reactions are known as hetero-Diels-Alder (HDA) reactions.

HDA reactions involving carbonyl compounds as hetero-dienes and/or hetero-dienophiles have made a number of substituted six-membered oxygen containing heterocycles, namely dihydropyrans accessible. This methodology assumes immense significance as this ring occurs as structural motiff in many biologically active natural products. However, carbonyl compounds as dienophiles are much less reactive and for their HDA reaction, often a Lewis acid is required as catalyst. This is possibly the reason why only a limited number of HDA reactions between the unactivated aldehydes and simple dienes have been reported so far.

The present studies were undertaken with a view to investigate HDA reactions of aromatic aldehydes with simple dienes (2,3-dimethyl-1,3-butadiene and isoprene) in the presence of Ti(IV) catalysts theoretically as well as experimentally. The results have been presented in the following four chapters:

Chapter 1 Hetero-Diels-Alder reaction of carbonyl compounds: A Review

Chapter 2 Hetero-Diels-Alder reaction of aromatic aldehydes catalyzed by titanium tetrachloride

Chapter 3 Asymmetric hetero-Diels-Alder reaction of aromatic aldehydes catalyzed by ((*R*)-1,1´-bi-2-naphthoxy)titanium dichloride

Chapter 4 Hetero-Diels-Alder reaction of aromatic aldehydes catalyzed by Lewis acids other than Ti(IV) – Theoretical and experimental results

Chapter 1 Hetero-Diels-Alder reaction of carbonyl compounds: A Review

An overview of the hetero-Diels-Alder reactions of the carbonyl compounds covering literature up to July 2015 has been presented in this chapter. It also includes a brief general introduction of the Diels-Alder (DA) reaction, its classification into normal electron demand (NED) and inverse electron demand (IED) cycloadditions and their Frontier Molecular Orbital (FMO) description. The mechanistic pathways followed by the HDA reaction, namely the concerted mechanism as well as the stepwise mechanism have also been outlined in this chapter.

Chapter 2 Hetero-Diels-Alder reaction of aromatic aldehydes catalyzed by titanium tetrachloride

This chapter has been divided into five sections

2.1 Introduction

The Hetero-Diels-Alder (HDA) reaction between aldehydes and dienes is restricted either to the reaction of highly electron-rich dienes with simple aldehydes or to the reaction of highly activated aldehydes with simple dienes. A limited number of HDA reactions between the unactivated aldehydes and simple dienes have been reported so far, which often requires a Lewis acid as catalyst. In view of this, we undertook a systematic experimental and theoretical investigation of the HDA reactions of aromatic aldehydes with simple dienes, namely 2,3-dimethyl-1,3-butadiene (DMB) and 2-methyl-1,3-butadiene (isoprene) in the absence and presence of titanium tetrachloride ($TiCl_4$) as catalyst.

2.2 Results and Discussion

2.2.1 Experimental Results

Aromatic aldehydes (**1**) react with 1,3-dienes (**2**) in the presence of $TiCl_4$ (15mol%) in toluene at room temperature under inert atmosphere to afford 3,6-dihydro-2*H*-pyran derivatives (**3**) (Scheme 2.2).

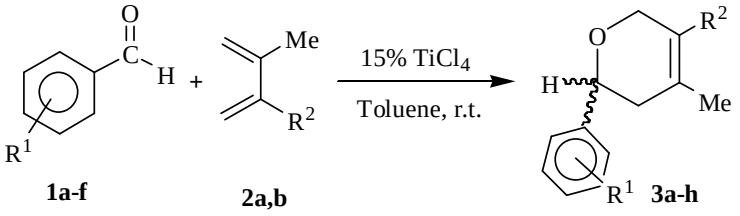

1a-f **2a,b** **3a-h**

1	R^1
a	3-NO_2
b	4-Cl
c	2-OMe
d	2,5-$(OMe)_2$
e	4-CF_3
f	3-CF_3

2	R^2
a	Me
b	H

3	R^1	R^2
a	3-NO_2	Me
b	4-Cl	Me
c	2-OMe	Me
d	2,5-$(OMe)_2$	Me
e	4-CF_3	Me
f	3-CF_3	Me
g	3-NO_2	H
h	4-Cl	H

Scheme 2.2

On carrying out the HDA reaction of **1** with isoprene (**2b**; R^2 = H), the reaction was fully regioselective leading to only one regioisomer having 1:4 orientation of O and Me. The reaction was found to be complete within 1-2.5 hrs. All the cycloadducts were pale yellow to orangish yellow syrupy mass and were soluble in polar as well as non-polar solvents.

Spectral Characterization

The structures of the cycloadducts have been established on the basis of IR and ^{1}H NMR and ^{13}C NMR spectroscopic techniques.

2.2.1.1 IR

In the IR spectra of **3a-h**, an intense absorption band due to cyclic C-O-C stretching vibration is observed in the range of υ 1107 - 1090 cm^{-1}. The aromatic skeletal vibrations give characteristic absorption bands in the range of υ 1531 - 1405

cm^{-1}. In **3a** and **3g,** two absorption bands at ~ υ 1455 cm^{-1} and ~ υ 1350 cm^{-1} are observed due to the asymmetric and symmetric N-O stretching vibrations respectively of the nitro group.

2.2.1.2 ^{1}H NMR

In the cycloadducts **3a-h,** the protons H_B and H_C (at C3) are diastereotopic and constitute an ABC spin system with the proton H_A (at C2). The proton H_B gives a double doublet (dd) at δ 2.91 - 2.11 ppm ($^{2}J_{HB,HC}$= 16.8 - 14.1Hz, $^{3}J_{HB,HA}$= 10.5 - 9.0 Hz), whereas a double doublet is observed at δ 3.06 – 2.12 ppm ($^{2}J_{HC,HB}$= 16.8 - 14.1 Hz, $^{3}J_{HC,HA}$= 6.0 - 3.6 Hz) for the proton H_C. Likewise, the proton H_A, gives a double doublet (dd) at δ 4.91 – 4.49 ppm ($^{3}J_{HA,HB}$= 10.5 – 9.0 Hz, $^{3}J_{HA,HC}$= 6.0 – 3.6 Hz). Similarly, protons H_D and H_E at C6 are diastereotopic forming an AB spin system and each gives a doublet at δ 4.35 - 4.18 ppm ($^{2}J_{HD,HE}$= 16.0 – 11.1 Hz) and at δ 4.35 - 4.05 ppm ($^{2}J_{HD,HE}$= 16.0 – 11.1 Hz) respectively. Two singlets in the region of δ 1.70 – 1.57 ppm are observed for the methyl protons at C4 and C5 for the products **(3a-f)** obtained from the reaction with DMB. In **3g** and **3h,** singlets at δ 1.77 ppm and δ 1.79 ppm are observed respectively for the methyl groups at C4. A singlet at ~5.50 is observed due to vinylic proton present at C4 for the products obtained from the reaction with isoprene. In **3c** and **3d** singlets at δ 3.82 ppm and δ 3.80 ppm respectively are assigned for the methoxy protons. The aromatic protons of the phenyl ring absorb in the region of δ 8.26 – 6.68 ppm.

2.2.1.3 ^{13}C NMR

In the ^{13}C NMR spectra, carbon atoms directly bonded to the oxygen atom, namely C2 and C6 absorb typically at δ 76.1 - 70.6 ppm and δ 70.7 - 70.1 ppm respectively. Signal of C3 appears in the range of δ 38.5 – 37.3 ppm. C4 and C5

carbon atoms give signals in more downfield region at δ 129.3 – 128.0 ppm and δ126.9 – 124.7 ppm respectively, the range characteristic for the vinylic carbon atoms. Carbon atoms of the methyl groups attached to C4 and C5 give signals at δ 18.8 – 17.2 ppm and δ 15.0 - 13.8 ppm respectively for the products obtained from the reaction with DMB. In **3g**, a peak at δ 22.9 ppm is observed for the carbon of the methyl group attached at C4.The aromatic carbons of the phenyl ring appear in the region of δ 155.8 – 110,2 ppm.

2.2.2 DFT investigation of the stereo and regio-selectivity

To investigate the mechanism of the HDA reactions of aromatic aldehydes (**4**) in the absence and the presence of $TiCl_4$, following nineteen model reactions were computed at the DFT (B3LYP/6-31G(d,p) level (Scheme 2.3).

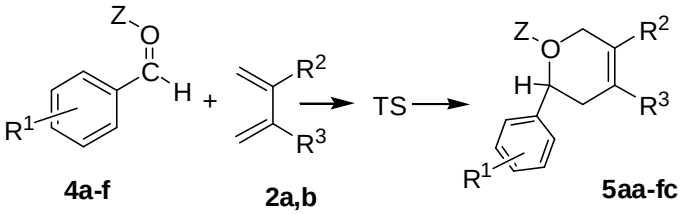

4a-f **2a,b** **5aa-fc**

4	Z	R^1
a	NIL	H
b	NIL	*p*-Cl
c	NIL	*o*-Me
d	$TiCl_4$	H
e	$TiCl_4$	*p*-Cl
f	$TiCl_4$	*o*-Me

2	R^2	R^3
a	Me	Me
b	Me	H

5	Z	R^1	R^2	R^3
aa	NIL	H	Me	Me
ab	NIL	H	Me	H
ac	NIL	H	H	Me
ba	NIL	*p*-Cl	Me	Me
bb	NIL	*p*-Cl	Me	H
bc	NIL	*p*-Cl	H	Me
ca	NIL	*o*-Me	Me	Me
cb	NIL	*o*-Me	Me	H
cc	NIL	*o*-Me	H	Me
da	$TiCl_4$	H	Me	Me
db	$TiCl_4$	H	Me	H
dc	$TiCl_4$	H	H	Me
ea	$TiCl_4$	*p*-Cl	Me	Me
eb	$TiCl_4$	*p*-Cl	Me	H
ec	$TiCl_4$	*p*-Cl	H	Me
fa	$TiCl_4$	*o*-Me	Me	Me
fb	$TiCl_4$	*o*-Me	Me	H
fc	$TiCl_4$	*o*-Me	H	Me

Scheme 2.3

The HDA reaction of **4a** with DMB **(2a)** has been computed for both *endo* and *exo* approaches of the diene. The *endo* approach is found to be more preferable over the *exo* approach by about 0.5 kcal mol^{-1}. Thus in other cases, only the transition structures for the *endo* approach have been investigated.

2.2.2.1 Optimized Geometries

This section incorporates representation of the optimized geometries (B3LYP/6-31G(d,p)), of various reactants, transition structures, intermediates and cycloadducts involved in the uncatalyzed and $TiCl_4$ catalyzed HDA reaction. Geometrical parameters, namely bond lengths (in Å) and Wiberg Bond Indices (WBI) for the selected bonds of the transition structures, intermediates and the products are also given.

The uncatalyzed HDA reactions are found to follow the pericyclic mechanism with asynchronous transition structures, where the newly forming C2–C3 bond (WBI = 0.45 – 0.48) is more advanced than the C6–O1 bond (WBI = 0.33 – 0.36). However, the $TiCl_4$ catalyzed HDA reaction of the aromatic aldehydes follows the stepwise mechanism in which the first step leading to the zwitterionic intermediate is rate determining. The formation of the C2–C3 bond in the first transition structure, **TS10(i)** is quite advanced (bond distance, 1.86Å; WBI, 0.59) and approaches to the reaction intermediate, **Int10**. The second transition state, **TS10(ii)** is not much different from the intermediate, i.e. it is reached quite early.

In order to rationalize the regioselectivity, both *para* and *meta* approaches have been investigated. For the uncatalyzed HDA reaction of the aromatic aldehydes with isoprene, the transition structures resulting from the *para* approach of the diene

(O/Me, 1:4) are comparatively more asynchronous (WBI, C2–C3 = ~ 0.46, C6–O1 = 0.33) than the transition structures of the corresponding *meta* approach (O/Me, 1:3) (WBI, C2–C3 = ~ 0.45, C6–O1 = ~ 0.36). In case of the $TiCl_4$ catalyzed HDA reaction with isoprene, the *para* product follows a stepwise mechanism whereas *meta* approach involves asynchronous concerted transition state.

Highly negative NICS(0) and NICS(1) values confirm the aromatic and the concerted nature of the transition structures involved in the uncatalyzed HDA reactions. The decreases in NICS(0) values for the TS of $TiCl_4$ catalyzed HDA reaction shows increase in asynchronicity as compared to the uncatalyzed reaction.

2.2.2.2 Energetics

The total energies and relative enthalpies (ΔH) for the HDA reactions 1-19 both in the gas phase as well as in toluene are presented in this section. The activation enthalpy ($\Delta H^{\neq}$) of the uncatalyzed HDA reaction of benzaldehyde with DMB in the gas phase ($\Delta H^{\neq}$= 29.72 kcal mol^{-1}) is quite high, which increases further by ca. 1 kcal mol^{-1} in toluene. It explains the inertness of aromatic aldehydes towards HDA reaction under uncatalyzed conditions.

The presence of $TiCl_4$ as catalyst lowers the $\Delta H^{\neq}$ by ~12 kcal mol^{-1} in the gas phase, which is further reduced in toluene by 2 kcal mol^{-1}. Although it has been possible to locate the second transition state, it is very similar to the intermediate and is only 0.11 kcal mol^{-1} higher in energy than the intermediate in the gas phase (0.46 kcal mol^{-1} in the solvent). The presence of EWG and EDG on benzaldehyde did not make significant change in the $\Delta H^{\neq}$ of the reaction.

Stereo- and regioselectivity

With respect to stereoselectivity, it was found that the activation enthalpies for the HDA reactions involving *endo* approach of the diene are lower by ~0.5 kcal mol^{-1} than its *exo* approach. As regards the regioselectivity of the reaction with isoprene in the presence of $TiCl_4$ catalyst, the path leading to the *para* regioisomer (O/Me, 1:4) has lower $\Delta H^{\neq}$ than the path giving *meta* regioisomer (O/Me, 1:3) by ~6 kcal mol^{-1}.

The regio-selectivities observed in the investigated HDA reactions have been rationalized by calculating ratio of the two regioisomers using the Boltzmann distribution equation. The calculated results indicate that the $TiCl_4$ catalyzed HDA reactions of aromatic aldehyde with isoprene should lead to >99% regioselectivity. Experimentally, $TiCl_4$ catalyzed HDA reactions are accompanied by 100% regioselectivity.

2.2.2.3 Global properties

The reactivity of aldehydes in their ground states have been investigated on the basis of the electrophilicity and nucleophilicity indices. According to it, $TiCl_4$ complex of aldehydes has higher electrophilic index than the corresponding uncomplexed aldehydes. Thus the complexed species is much more reactive electrophile. Thus, the $TiCl_4$ catalyzed HDA reactions are found to occur through a more polar and stepwise mechanism, as compared to the uncatalyzed process.

2.2.2.4 NBO Analysis:

The NBO analysis reveals the co-ordination of $TiCl_4$ to the oxygen atom of the carbonyl group by the second order perturbation interactions between LP_{O1} to LP^*_{Ti} with high second order perturbation energy values (~ 20 kcal mol^{-1}). In the

$TiCl_4$catalyzed HDA reactions with DMB, the newly formed bond interacts strongly with other bonds in the ring by σ_{C2-C3} to LP^*_{C4}, π_{C5-C6} to LP^*_{C4}, LP_{O1} to σ^*_{C2-C3}, LP_{C4} to σ^*_{C2-C3}, and LP_{C4} to π^*_{C5-C6}, effective interactions, which shows complete delocalization of the electrons in the transition structures (TSi, TSii) and intermediate.

2.2.2.5 FMO Analysis

An inspection of the FMOs shows that complexation with $TiCl_4$ not only lowers energy of the LUMO of benzaldehyde, it also causes its polarization. The lobe on the carbonyl oxygen atom is merged with the d orbital of the titanium atom by d_π-p_π bonding due to which carbonyl carbon becomes significantly positively charged and shifts the reaction from the concerted to the stepwise ionic mechanism.

2.3 Experimental Details

Various techniques and procedures used during the HDA reaction of aromatic aldehydes with DMB or isoprene in the presence of $TiCl_4$ are given in this section.

2.4 Computational Details

Various computational techniques used during the theoretical investigation of the HDA reactions have been described in this section.

2.5 Conclusions

The HDA reactions of aromatic aldehydes **(1)** with simple dienes such as DMB (**2a**) and isoprene (**2b**) could be accomplished successfully in the presence of 15 mol% $TiCl_4$ to give 3,6-dihydro-2*H*-pyrans (**3**) derivatives in high yields. Theoretical investigation of the HDA reactions of the aromatic aldehydes with simple dienes revealed that in the absence of a catalyst, the activation enthalpies are high explaining the non-occurrence of the reactions under these conditions. However, the

activation enthalpies of the $TiCl_4$ catalyzed reactions are lowered remarkably making the occurrence of these reactions feasible. Furthermore, under these conditions, reactions follow a stepwise ionic mechanism involving a zwitterionic intermediate. The activation enthalpies involving *endo* approach of the diene are lower than that of the *exo*-isomers by ~0.5 kcal mol^{-1}. The reaction with isoprene is expected to take place with complete regioselectivity to give the regioisomer having O/Me in the 1:4 positions.

Chapter 3 Asymmetric hetero-Diels-Alder reaction of aromatic aldehydes catalyzed by ((*R*)-1,1´-bi-2-naphthoxy)titanium dichloride

This chapter has been divided into six sections

3.1 Introduction

After having succeeded in carrying out the HDA reaction of aromatic aldehydes with simple dienes (2,3-dimethyl-1,3-butadiene (DMB) and isoprene) catalyzed by titanium tetrachloride ($TiCl_4$), we were motivated to explore asymmetric HDA reaction using an appropriate chiral Ti(IV) catalyst. In view of this, we investigated asymmetric HDA reactions of aromatic aldehydes with DMB catalyzed by ((*R*)-1,1´-bi-2-naphthoxy)titanium dichloride experimentally and theoretically.

3.2 Experimental Results

The HDA reaction of aromatic aldehydes **(1)** with DMB **(2)** were carried out by using ((*R*)-1,1´-bi-2-naphthoxy)titanium dichloride **(3)** as catalyst in toluene at ~ -15°C under inert atmosphere in the presence of molecular sieves (MS) 4Å to afford cycloadducts (3,6-dihydro-4,5-dimethyl-2*H*-pyrans, **4**) (Scheme 3.1). Catalyst **3** was

generated in situ by reacting (*R*)-1,1´-bi-2-naphthol with bis-(isopropoxy)titanium dichloride ($Ti(O^iPr)_2Cl_2$) in the presence of MS (4Å).

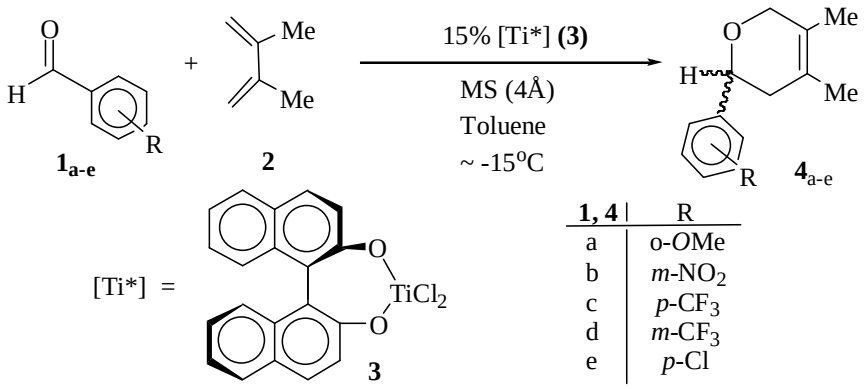

1, 4	R
a	o-*O*Me
b	*m*-NO_2
c	*p*-CF_3
d	*m*-CF_3
e	*p*-Cl

Scheme 3.1

All the products **(4)** were obtained as yellow to orangish yellow syrupy mass, soluble in polar as well as non-polar solvents. The structures of the products were established with the help of the extensive spectroscopic techniques (IR, ^1H and ^{13}C NMR).

3.2.1 Spectral Characterization

3.2.1.1 IR

In the cycloadduct **4**, an intense absorption band is observed in the range of υ 1107 - 1090 cm^{-1} due to C-O-C stretching vibration. The characteristic absorption bands for the aromatic skeletal vibrations appear in the range of υ 1531 - 1405 cm^{-1} and υ 1599 - 1583 cm^{-1}.

3.2.1.2 ^1H NMR

In the ^1H NMR spectra of the cycloadduct **4**, the aromatic protons of the phenyl ring absorb in the region of δ 8.26 – 6.68 ppm. The protons H_B and H_C (at C3) are diastereotopic and constitute an ABC spin system with the proton H_A (at C2). They appear as two double doublets in the regions of δ 2.91 - 2.11 ppm ($^2J_{HB,HC}$=

16.8- 14.1Hz, $^{3}J_{HA,HB}$= 10.5 - 9.0 Hz) and δ 3.06 – 2.11 ppm ($^{2}J_{HB,HC}$= 16.8 - 14.1 Hz, $^{3}J_{HA,HC}$= 6.0 - 3.6 Hz) respectively.. A double doublet (dd) for proton H_A is observed in the range of δ 4.91 – 4.49 ppm ($^{3}J_{HA,HB}$= 10.5 – 9.0 Hz, $^{3}J_{HA,HC}$= 6.0 – 3.6 Hz), Likewise, protons H_D and H_E at C6 are diastereotopic forming an AB spin system and each gives a doublet at δ 4.35 - 4.18 ppm ($^{2}J_{HD,HE}$= 16.0 – 11.1 Hz) and δ 4.35 - 4.05 ppm ($^{2}J_{HD,HE}$= 16.0 – 11.1 Hz) respectively. Two singlets are observed in the region of δ 1.70 – 1.57 ppm for the methyl groups protons at C4 and C5. In the case of **4a,** a singlet at δ 3.82 ppm is assigned to the OMe group at C2′.

3.2.1.3 ^{13}C NMR

In the ^{13}C NMR spectra of **4**, the aromatic carbons of the phenyl ring appear in the region of δ 155.8 – 110,2 ppm. The carbon atoms C2 and C6 directly bonded to the oxygen atom absorb typically at δ 77.1 - 70.6 ppm and δ 70.7 - 70.1 ppm respectively. Signal of C3 appears in the range of δ 38.6 – 37.4 ppm. The signals of C4 and C5 carbon atoms are observed in the downfield region at δ 129.3 – 128.0 ppm and δ 126.9 – 124.7 ppm respectively. Carbon atoms of the methyl groups attached on C4 and C5 give signals at δ 18.8 – 17.2 ppm and δ 15.0 - 13.8 ppm respectively.

3.2.2 Enantiomeric Excess:

The enantiomeric excess (*ee*) was analyzed by high performance liquid chromatography (HPLC) method using chiral OJ-H column. The reactions proceeded with good enantioselectivity which ranges from 68 to 95%, the highest being in the DA reaction of *o*-methoxybenzaldehyde.

3.3 DFT investigation of the stereoselectivity of the asymmetric hetero-Diels-Alder reaction

Results and Discussion

In contrast to the successful computational calculations of Ti(IV) chloride catalyzed DA reaction of aromatic aldehydes with DMB at the B3LYP/6-31G(d,p) level reported in the previous chapter, the calculations in the present case at the same level turned out to be computationally quite expensive and often tripped. Then we compared the enthalpies obtained at the B3LYP/6-31G(d,p) and B3LYP/STO-3G levels for the reactions reported in the previous chapter. It was found that the activation enthalpies at the B3LYP/STO-3G level were underestimated as compared to those at the B3LYP/6-31G(d,p) level by 12-16 kcal mol^{-1}; however, this difference was almost consistent. From this, we concluded that the difference between the activation enthalpies for the attacks by DMB on the *Si* and *Re* faces of the ((*R*)-1,1´-bi-2-naphthoxy)titanium dichloride complex of the aldehyde will not be significantly different at the B3LYP/STO-3G level from that at the B3LYP/6-31G(d,p) level. With this background, in the present case we computed following model reactions in the gas and solvent (toluene) phases at the B3LYP/STO-3G level (Scheme 3.3).

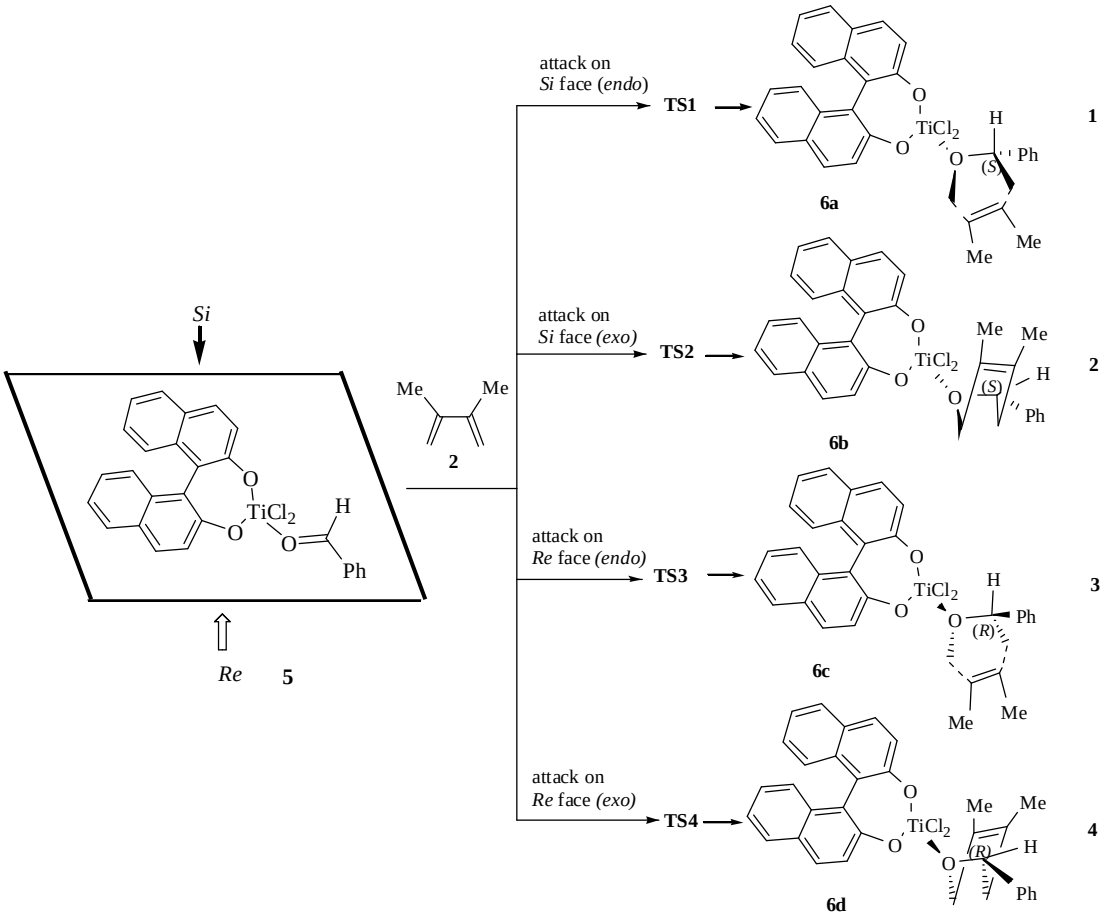

Scheme 3.3

The optimized geometries of the reactants [((*R*)-1,1´-bi-2-naphthoxy)titanium dichloride] complex of benzaldehyde has two faces, namely *Re* and *Si* for the reaction involving the >C=O functionality. The results of the computational calculations of the *Re*/*Si* face attack in *endo*/*exo* approach of HDA reaction are presented in this section.

3.3.1 Optimized Geometries

This section incorporates optimized geometries (B3LYP/6-31G(d,p)), of the reactants, cycloadducts, and their corresponding transition structures involving *Re*/*Si* face attacks in *endo*/*exo* approach. Various structural parameters, namely bond distances along their WBI, bond angles and dihedral angles of the selected bonds of all the stationary points are also given.

3.3.2 Energetics

The relative activation enthalpies ($\Delta H^{\neq}$) and the reaction enthalpies ($\Delta H°$), with respect to the total energies of the reactants in both gas phase as well as in toluene have been calculated at B3LYP/6-31G(d,p).

The cycloaddition reaction of **5** with **2** involving attack from the *Si* face of the >C=O functionality has lower activation barrier. The activation barrier involving attack of the diene in the *endo* manner from the *Si* face (TS1) is lower in energy by 1.87 kcal mol^{-1} in the gas phase and 1.37 kcal mol^{-1} in the toluene as compared to those for the attack from the *Re* face (*endo*) (TS3). However for the reaction of **5** with DMB involving attack of the diene from the *Si* face, (reaction 2), the activation energy barrier for the *exo* approach involving TS2 is smaller (reaction 2) than the *endo* approach via TS1 (reaction 1) by 0.73 kcal mol^{-1}.

The relative Gibbs energy also favors *exo* approach over the *endo* approach from the *Si* face.

3.4 Experimental Details

Various procedures and techniques used during the asymmetric HDA reaction of aromatic aldehydes with DMB in the presence of chiral Ti(IV) catalyst are given in this section.

3.5 Computational Details

The methods of computational calculations and details of the supporting software used during the theoretical investigation of HDA reaction have been described in this section.

3.6 Conclusions

The HDA reactions of aromatic aldehydes **(1)** with DMB **(2)** have been accomplished successfully in the presence of 15 mol% ((*R*)-1,1´-bi-2-naphthoxy)titanium dichloride **(3)** as catalyst to give 3,6-dihydro-2*H*-pyran derivatives **(4)** in 37-74% yields with good to high enantioselectivies (68-95 *ee*). Computational calculations of the model HDA reactions at the DFT (B3LYP/STO-3G) level reveal that attack of the diene occurs preferentially from the *Si* face of the aldehydes-catalyst complex **(5)**, with marginal *exo* selectivity.

Chapter 4 Hetero-Diels-Alder reaction of aromatic aldehydes catalyzed by Lewis acids other than Ti(IV) – Theoretical and experimental results

4.1 Introduction

In this chapter, theoretical results of the catalytic activity of other Lewis acids, namely aluminium chloride, ethylaluminium dichloride, boron trifluoride and zinc chloride vis-à-vis HDA reaction of the aromatic aldehydes with DMB and isoprene are presented. Besides, this chapter also incorporates the experimental results of the HDA reactions of aromatic aldehydes in the presence of $EtAlCl_2$ as catalyst.

4.2 DFT investigation of the catalytic activity of Lewis acids on the HDA reaction of aromatic aldehydes

Results and Discussion

The following twelve model reactions in the gas and solvent (toluene) phases were computed at the DFT (B3LYP/6-31G(d,p)) level (Scheme 4.1).

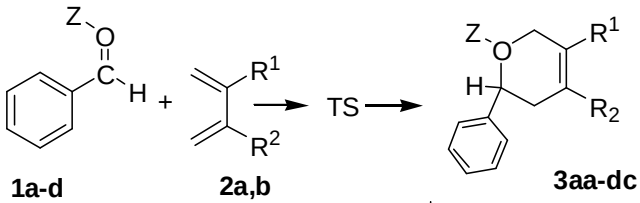

1a-d

1	Z
a	$AlCl_3$
b	$EtAlCl_2$
c	BF_3
d	$ZnCl_2$

2a,b

2	R^1	R^2
a	Me	Me
b	Me	H

3aa-dc

3	Z	R^1	R^2
aa	$AlCl_3$	Me	Me
ab	$AlCl_3$	Me	H
ac	$AlCl_3$	H	Me
ba	$EtAlCl_2$	Me	Me
bb	$EtAlCl_2$	Me	H
bc	$EtAlCl_2$	H	Me
ca	BF_3	Me	Me
cb	BF_3	Me	H
cc	BF_3	H	Me
da	$ZnCl_2$	Me	Me
db	$ZnCl_2$	Me	H
dc	$ZnCl_2$	H	Me

Scheme 4.1

4.2.1 Optimized Geometries

Structural features of the optimized geometries of the stationary points, namely reactants (**1a-d**), transition structures (**TS1-12**) and cycloadducts (**3aa-3dc**) on the PES of the HDA reactions 1-12 are described in this section.

All the transition structures are found to be asynchronous where the newly forming C2–C3 bond (WBI= 0.60 – 0.70) is more advanced than the C6–O1 bond (WBI = 0.06 – 0.18). It was found that the transition structures in the presence of $AlCl_3$ (WBI C2-C3= 0.61, WBI O1-C6= 0.07) and $EtAlCl_2$ (WBI C2-C3= 0.64, WBI O1-C6= 0.08) are more asynchronous than the transition structures involved in the HDA reactions catalyzed by BF_3 (WBI C2-C3= 0.65, WBI O1-C6= 0.12) and $ZnCl_2$ (WBI C2-C3= 0.67, WBI O1-C6= 0.18). Thus the order of asynchronicity in the catalyzed HDA reaction was found to be

Uncatalyzed < $ZnCl_2$< BF_3 < $AlCl_3$< $EtAlCl_2$

Thus the results obtained from the HDA reactions catalyzed by any of the above catalysts are in contrast to the HDA reactions catalyzed by Ti(IV) chloride, because the latter follows stepwise mechanism,

As regard the regioselectivity in the reaction with isoprene, a similar trend was observed in the all cases, the transition structures resulting from the *para* approach of the diene (O/Me, 1:4) are comparatively more asynchronous (WBI C2-C3= 0.62 – 0.67, WBI O1-C6 = 0.07 – 0.16) than the transition structures involved in the *meta* approach (O/Me, 1:3) (WBI C2-C3 = 0.63 – 0.73, WBI O1-C6 = 0.15 – 0.22).

NICS values

The aromatic nature of the transition structures was confirmed by the highly negative NICS(0) and NICS(1) values, calculated at the (3,+1) ring critical points and the points 1 Å above the critical point respectively.

4.2.2 Energetics

This section includes total energies and relative enthalpies (ΔH) for the HDA reactions 1-12, in the gas and in solvent (toluene) phases.

The activation enthalpy ($\Delta H^{\neq}$) of the uncatalyzed HDA reaction of benzaldehyde is very high which comes down in the presence of a Lewis acid, $AlCl_3$, $EtAlCl_2$, BF_3, or $ZnCl_2$ to 12.26, 14.34, 14.59 and 18.82 kcal mol^{-1} respectively. Thus the order of activation enthalpies ($\Delta H^{\neq}$) in the presence of different catalysts is:

$$\mathbf{AlCl_3 < EtAlCl_2 \simeq BF_3 < ZnCl_2 << uncatalyzed}$$

For The HDA reactions with isoprene, the path leading to the *para* regioisomer has lower activation enthalpy than the respective *meta* regioisomer with more than 97% regioselectivity in the all cases.

4.2.3 Analysis of the global reactivity indices

The electrophilicity and nucleophilicity indices used to explain the electronic activation of the reagents involved in the polar DA reactions are discussed in this section. Co-ordination of a Lewis acid to the carbonyl oxygen atom of benzaldehyde increases the electrophilicity of the complexes, **1a-1d** (ω = 2.94 – 4.08 eV), which entails the increase of the ionicity of the process and decrease of the activation enthalpy of the reaction. The order of global electrophilicity (ω) is:

Uncatalyzed << $ZnCl_2$< BF_3 < $EtAlCl_2$ < $AlCl_3$

4.2.4 FMO Analysis:

The FMOs of benzaldehyde-Lewis acid complexes, **1a-1d** obtained at B3LYP/6-31G(d,p) level are discussed in this section. The co-ordination of Lewis acids with the lone pair on the carbonyl group of benzaldehyde lowers energy of its LUMO. Thus, the energy gap between the $HOMO_{diene}$ and $LUMO_{dienophile}$ is reduced compared to that in the absence of the Lewis acid and can therefore account for activating effect of the Lewis acid. It is noteworthy that polarization of the LUMO centred on the carbonyl group of benzaldehyde is not much altered after its complexation with the Lewis acids, which explains the involvement of a concerted transition state in all these cases.

4.3 HDA reaction of aromatic aldehydes catalyzed by $EtAlCl_2$

Encouraged by the above theoretical results, we investigated the HDA reactions of aromatic aldehydes (**4**) with DMB (**2a**) catalyzed by $EtAlCl_2$ experimentally.

4.3.1 Results and Discussion

The hetero-Diels-Alder reaction of aromatic aldehydes (**4**) with DMB (**2a**) in the presence of $EtAlCl_2$ (15 mol%) in toluene at room temperature under inert atmosphere affords 3,6-dihydro-4,5-dimethyl-2*H*-pyran derivatives (**5**) (Scheme 4.2).

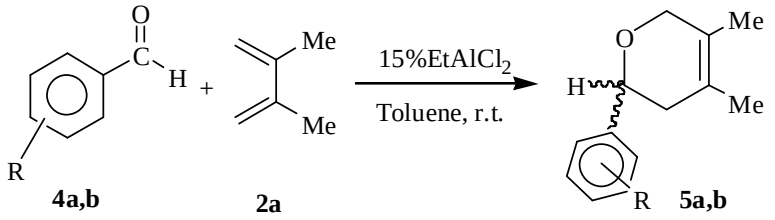

4a,b **2a** **5a,b**

4, 5	R
a	4-Cl
b	3-NO_2

Scheme 4.2

The progress of the reaction was monitored by thin layer chromatography (TLC) and it was observed that the reaction was complete in about 1-1.5 hrs at r.t. All the cycloadducts (**5**) were pale yellow to orangish yellow syrupy mass, soluble in polar as well as non-polar solvents.

4.3.2 Spectral Characterization

The structures of cycloadducts **5** were elucidated on the basis of IR, ^{1}H NMR and ^{13}C NMR studies.

4.3.2.1 IR

In the IR spectra of **5**, an intense absorption band due to cyclic C-O-C is observed at ~ υ 1100 cm^{-1}. The characteristic peaks of aromatic C=C and alkenyl C_4=C_5 are observed in the range of υ 1531 - 1405 cm^{-1} and υ 1600 - 1583 cm^{-1} respectively. In **5b,** two absorption bands at υ 1455 cm^{-1} and υ 1350 cm^{-1} are observed due to the sym. and asym. N-O stretching vibrations of the nitro group.

4.3.2.2 ^{1}H NMR

In the cycloadducts **5**, the aromatic protons of phenyl rings absorb in the region of δ 8.26 – 7.47 ppm. The protons H_B and H_C (at C3) are diastereotopic and constitute an ABC spin system with the proton H_A (at C2). The proton H_B gives a double doublet (dd) at δ 2.63 - 2.11 ppm ($^{2}J_{HB,HC}$= 15.6 Hz $^{3}J_{HB,HA}$= 9.9 Hz), whereas a double doublet is observed at δ 3.06 – 2.17 ppm ($^{2}J_{HC,HB}$= 15.6 Hz, $^{3}J_{HC,HA}$= 6.0 Hz) for the proton H_C. Likewise, the proton H_A, gives a double doublet (dd) at δ 4.65 – 4.49 ppm ($^{3}J_{HA,HB}$= 9.9 Hz, $^{3}J_{HA,HC}$= 6.0 Hz). Similarly, protons H_D and H_E at C6 are diastereotopic forming an AB spin system and each gives a doublet at δ 4.23 – 4.18 ppm ($^{2}J_{HD,HE}$= 15.6 Hz) and at δ 4.18 - 4.08 ppm ($^{2}J_{HD,HE}$= 15.6 Hz) respectively. Two singlets in the region of δ 1.70 – 1.57 ppm are observed for the methyl protons at C4 and C5.

4.3.2.3 ^{13}C NMR

In the ^{13}C NMR spectra of **5**, the aromatic carbons of the phenyl ring appear in the region of δ 144.9 – 121.0 ppm. The carbon atoms directly bonded to the oxygen atom, namely C2 and C6 absorb typically at ~ δ 75.0 ppm and ~ δ 70.5 ppm respectively. Signal of C3 appears in the range of δ 38.5 – 38.3 ppm. C4 and C5 carbon atoms give signals in more downfield region at δ 129.3 – 128.0 ppm and δ 126.9 – 124.7 ppm respectively. Carbon atoms of the methyl groups attached to C4 and C5 give signals at δ 18.8 – 18.3 ppm and δ 13.9 – 13.8 ppm respectively.

4.4 Computational and Experimental Details

4.4.1 Computational Details

Various computational techniques and supporting software used during the investigations have been described in this section.

4.4.2 Experimental Details

Various procedures and techniques used during the HDA reaction of aromatic aldehydes with DMB in the presence of $EtAlCl_2$ catalyst are given in this section

4.5 Conclusions

We have demonstrated theoretically that on using a Lewis acid viz. $AlCl_3$, $EtAlCl_2$, BF_3, or $ZnCl_2$, activation enthalpy of the HDA reaction of benzaldehyde with the dienes, DMB and isoprene is lowered substantially making occurrence of the reaction feasible. In all these cases, the reaction follows a concerted mechanism with asynchronous transition structures. The order of activation barrier is **$AlCl_3$< $EtAlCl_2$≃BF_3< $ZnCl_2$<< uncatalyzed.** This order can be rationalized on the basis of the electrophilicity order of the benzaldehyde-complexes with the respective Lewis acid.

During the reaction with isoprene, complete regioselectivity was observed where the major regioisomer has O/Me in the 1:4 position.

The above theoretical results could be verified by accomplishing successfully HDA reactions of aromatic aldehydes with DMB in the presence of 15mol% $EtAlCl_2$ to give 3,6-dihydro-4.5-dimethyl-2*H*-pyran derivatives in good yield.